UC Berkeley
UC Berkeley Previously Published Works

Title

Hidden pion varieties in composite models for diphoton resonances

Permalink

Journal

ISSN

Authors

Harigaya, Keisuke
Nomura, Yasunori

Publication Date

DOI

Hidden pion varieties in composite models for diphoton resonances

Keisuke Harigaya and Yasunori Nomura

Berkeley Center for Theoretical Physics, Department of Physics,
University of California, Berkeley, California 94720, USA
and Theoretical Physics Group, Lawrence Berkeley National Laboratory, Berkeley, California 94720, USA

The diphoton excesses at 750 GeV seen in the LHC data may be the first hint of new physics at the TeV scale. We discuss variations of the model considered earlier, in which one or more diphoton excesses arise from composite pseudo-Nambu-Goldstone bosons (hidden pions) associated with new strong dynamics at the TeV scale. We study the case in which the 750 GeV excess arises from a unique hidden pion leading to a diphoton final state as well as the case in which it arises from one of the hidden pions decaying into diphotons. We consider $SU(N)$, $SO(N)$, and $Sp(N)$ gauge groups for the strong dynamics and find that $SO(N)$ and $Sp(N)$ models give extra hidden pions beyond those in the $SU(N)$ models, which can be used to discriminate among models.

I. INTRODUCTION

The recently announced diphoton excess at $\simeq$750 GeV [1–4] may be the first hint of physics beyond the standard model at the TeV scale. In Ref. [5], we have proposed, based on stability of the theory and the strength of the signal, that this excess results from a composite spin-0 particle decaying into a two-photon final state. In Ref. [6], we have studied a particularly simple version of this, in which the 750 GeV particle is a composite pseudo-Nambu-Goldstone boson associated with new strong dynamics at the TeV scale which is singly produced by gluon fusion and decays into two photons. In particular, we have studied a model that has an extra gauge group $G_H = SU(N)$ at the TeV scale, in addition to the standard model gauge group $G_{SM} = SU(3)_C \times SU(2)_L \times U(1)_Y$, with extra matter—hidden quarks—in the vectorlike bifundamental representation of G_H and $SU(5) \supset G_{SM}$. We have studied detailed phenomenology of pseudo-Nambu-Goldstone bosons—hidden pions—one of which is the 750 GeV diphoton resonance. A class of theories involving similar dynamics with vectorlike matter charged under both hidden and standard model gauge groups was studied in Ref. [7]. The possibility of obtaining standard model dibosons from a composite scalar particle was utilized in a different context in Ref. [8]. For related work explaining the diphoton excess using similar dynamics, see Refs. [9–11].

In this paper, we study two classes of variations of the minimal model in Refs. [5,6]. For definiteness, we keep the G_{SM} quantum numbers of the hidden quarks to be $\mathbf{5} + \mathbf{5}^*$ of $SU(5) \supset G_{SM}$ motivated by grand unification. [Note that $SU(5)$ here is used as a mnemonic; it does not mean that the three factors of G_{SM} are actually unified at the TeV scale.] This provides the simplest way of preserving gauge coupling unification at the level of the standard model, which is significant given possible threshold corrections

around the TeV and unification scales; see, e.g., Ref. [12]. The unification of the couplings becomes even better if we introduce supersymmetry slightly above the TeV scale. In the first class, we consider models in which a single diphoton resonance arises from a unique G_{SM}-singlet hidden pion. After reviewing the $G_H = SU(N)$ model in Refs. [5,6], we discuss models with $G_H = SO(N)$ and $Sp(N)$. Other than being possible variations, these models have an additional motivation that the matter content is consistent with simple $SO(10)$ grand unified theories. We study symmetry breaking patterns and hidden pion contents, and we predict the spectra of hidden pions under the condition that the G_{SM}-singlet hidden pion is responsible for the 750 GeV excess. We find that $SO(N)$ and $Sp(N)$ models have extra hidden pions beyond those in the $SU(N)$ model, which can be used to discriminate among models. In fact, in terms of the hidden pion phenomenology, the models discussed here essentially cover all possibilities with the hidden quarks in a single representation of G_H and $\mathbf{5} + \mathbf{5}^*$ of $SU(5) \supset G_{SM}$. In the second class, we consider models in which multiple (two) diphoton resonances arise from hidden pions. In Ref. [6], it was found that this can occur if the model contains an extra hidden quark that is charged under G_H but singlet under G_{SM}. (Introduction of such an extra hidden quark was motivated by cosmology there.) We study $G_H = SU(N)$, $SO(N)$, and $Sp(N)$ models in this class. We demonstrate how parameters of the models are determined and how other G_{SM}-charged hidden pion masses are predicted once the two diphoton resonances are observed.

The composite models we discuss contain would-be stable particles which do not decay solely by G_H or G_{SM} gauge interactions. If they are electrically or color charged, their lifetimes must be short enough to evade cosmological constraints. The cosmological constraints and decays of would-be stable particles are discussed in Ref. [6] for

$G_H = SU(N)$. We extend these analyses to the case of $SO(N)$ and $Sp(N)$.

The organization of this paper is as follows. In Sec. II, we discuss models in which a single diphoton resonance arises from hidden pions. Models with $G_H = SU(N)$, $SO(N)$, and $Sp(N)$ are considered in three subsections. In Sec. III, we discuss models in which two diphoton resonances arise from hidden pions. Again, models with $G_H = SU(N)$, $SO(N)$, and $Sp(N)$ are considered. In Sec. IV, we discuss cosmological constraints and decays of the would-be stable particles. Section V gives a summary.

II. MINIMAL MODELS FOR THE 750 GEV RESONANCE

Here we discuss variations of the minimal model in Refs. [5,6]. After reviewing the salient features of the model in Sec. II A, we present variations in which the hidden gauge group is changed from $SU(N)$ to $SO(N)$ and $Sp(N)$ in Secs. II B and II C, respectively. We discuss the symmetry breaking pattern and hidden pion spectrum in each case. We find that the $SO(N)$ and $Sp(N)$ models have extra hidden pions beyond those in the $SU(N)$ case.

A. $G_H = SU(N)$

The model has a hidden gauge group $G_H = SU(N)$, with dynamical scale $\Lambda \approx O(\text{TeV})$, and hidden quarks charged under both G_H and the standard model gauge groups, G_{SM}, as in Table I.[1] Here, we assume $N \geq 3$; the case of $G_H = SU(2)$ [$\simeq Sp(2)$] is analyzed in Sec. II C. The hidden quarks have mass terms

$$\mathcal{L} = -m_D \Psi_D \bar{\Psi}_D - m_L \Psi_L \bar{\Psi}_L + \text{H.c.,} \qquad (1)$$

where we take $m_{D,L} > 0$ without loss of generality, and we assume $m_{D,L} \lesssim \Lambda$. Note that the charge assignment of the hidden quarks is such that they are a vectorlike fermion in the bifundamental representation of G_H and $SU(5) \supset G_{\text{SM}}$, so that the model preserves gauge coupling unification at the level of the standard model. Throughout the paper, we assume that the hidden sector preserves CP to a good accuracy.

The strong G_H dynamics makes the hidden quarks condensate

$$\langle \Psi_D \bar{\Psi}_D + \Psi_D^\dagger \bar{\Psi}_D^\dagger \rangle \approx \langle \Psi_L \bar{\Psi}_L + \Psi_L^\dagger \bar{\Psi}_L^\dagger \rangle \equiv -c. \qquad (2)$$

These condensations do not break the standard model gauge groups, but they break the approximate $SU(5) \times SU(5)$ flavor symmetry of the G_H gauge theory to the diagonal $SU(5)$ subgroup. The spectrum below Λ,

TABLE I. Charge assignment of the minimal model with $G_H = SU(N)$. Here, $\Psi_{D,L}$ and $\bar{\Psi}_{D,L}$ are left-handed Weyl spinors. We denote representations of G_H by a Young tableaux while those of G_{SM} by the dimensions of representations.

	$G_H = SU(N)$	$SU(3)_C$	$SU(2)_L$	$U(1)_Y$
Ψ_D	□	$\mathbf{3}^*$	$\mathbf{1}$	$1/3$
Ψ_L	□	$\mathbf{1}$	$\mathbf{2}$	$-1/2$
$\bar{\Psi}_D$	$\bar{\square}$	$\mathbf{3}$	$\mathbf{1}$	$-1/3$
$\bar{\Psi}_L$	$\bar{\square}$	$\mathbf{1}$	$\mathbf{2}$	$1/2$

therefore, consists of 24 hidden pions, whose quantum numbers under $G_{\text{SM}} = SU(3)_C \times SU(2)_L \times U(1)_Y$ are

$$\psi(\mathbf{8}, \mathbf{1})_0, \quad \chi(\mathbf{3}, \mathbf{2})_{-5/6}, \quad \varphi(\mathbf{1}, \mathbf{3})_0, \quad \phi(\mathbf{1}, \mathbf{1})_0, \qquad (3)$$

where ψ, φ, and ϕ are real scalars while χ is a complex scalar. The masses of these particles are given by

$$m_\psi^2 = 2m_D \frac{c}{f^2} + 3\Delta_C, \qquad (4)$$

$$m_\chi^2 = (m_D + m_L)\frac{c}{f^2} + \frac{4}{3}\Delta_C + \frac{3}{4}\Delta_L + \frac{5}{12}\Delta_Y, \qquad (5)$$

$$m_\varphi^2 = 2m_L \frac{c}{f^2} + 2\Delta_L, \qquad (6)$$

$$m_\phi^2 = \frac{4m_D + 6m_L}{5}\frac{c}{f^2}. \qquad (7)$$

Here, f is the decay constant,[2] and $\Delta_{C,L,Y}$ are contributions from standard model gauge loops of order

$$\Delta_C \simeq \frac{3g_3^2}{16\pi^2}\Lambda^2, \quad \Delta_L \simeq \frac{3g_2^2}{16\pi^2}\Lambda^2, \quad \Delta_Y \simeq \frac{3g_1^2}{16\pi^2}\Lambda^2, \qquad (8)$$

where g_3, g_2, and g_1 are the gauge couplings of $SU(3)_C$, $SU(2)_L$, and $U(1)_Y$, respectively, with g_1 in the $SU(5)$ normalization. Using naive dimensional analysis [14], we can estimate the quark bilinear condensate and the decay constant as

$$c \approx \frac{N}{16\pi^2}\Lambda^3, \qquad f \approx \frac{\sqrt{N}}{4\pi}\Lambda. \qquad (9)$$

The couplings of the hidden pions with the standard model gauge fields are determined by chiral anomalies and given by

---

[1]Throughout the paper, we adopt the hypercharge normalization such that the standard model left-handed Weyl fermions have $(q, u, d, l, e) = (1/6, -2/3, 1/3, -1/2, 1)$.

[2]Our definition of the decay constant f is a factor of 2 different from that in Ref. [13]: $f = F/2$.
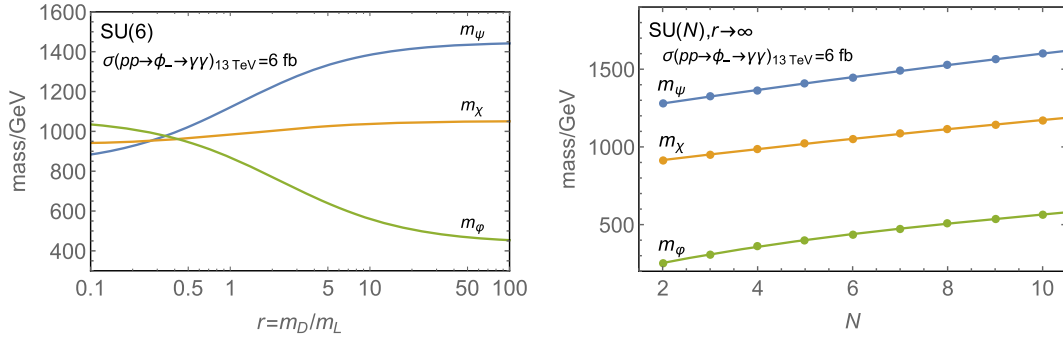
FIG. 1.   The masses of hidden pions ψ, χ, and φ for $m_\phi = 750$ GeV as functions of $r = m_D/m_L$ for $N = 6$ (left) and as functions of N for $r \to \infty$ (right).

$$\mathcal{L} = \frac{Ng_3^2}{64\pi^2 f} d^{abc} \psi^a \epsilon^{\mu\nu\rho\sigma} G_{\mu\nu}^b G_{\rho\sigma}^c + \frac{Ng_3 g_1}{16\sqrt{15}\pi^2 f} \psi^a \epsilon^{\mu\nu\rho\sigma} G_{\mu\nu}^a B_{\rho\sigma}$$
$$- \frac{3Ng_2 g_1}{32\sqrt{15}\pi^2 f} \varphi^\alpha \epsilon^{\mu\nu\rho\sigma} W_{\mu\nu}^\alpha B_{\rho\sigma} + \frac{Ng_3^2}{32\sqrt{15}\pi^2 f} \phi \epsilon^{\mu\nu\rho\sigma} G_{\mu\nu}^a G_{\rho\sigma}^a$$
$$- \frac{3Ng_2^2}{64\sqrt{15}\pi^2 f} \phi \epsilon^{\mu\nu\rho\sigma} W_{\mu\nu}^\alpha W_{\rho\sigma}^\alpha - \frac{Ng_1^2}{64\sqrt{15}\pi^2 f} \phi \epsilon^{\mu\nu\rho\sigma} B_{\mu\nu} B_{\rho\sigma}, \qquad (10)$$

where $a, b, c = 1, \dots, 8$ and $\alpha = 1, 2, 3$ are $SU(3)_C$ and $SU(2)_L$ adjoint indices, respectively, and $d^{abc} \equiv 2\mathrm{tr}[t^a \{t^b, t^c\}]$ with t^a being half of the Gell-Mann matrices. Assuming that the ϕ particle produced by gluon fusion and decaying to a diphoton is responsible for the 750 GeV excess, we find that the diphoton rate and $m_\phi \simeq 750$ GeV determine the parameters of the model as [6]

$$f \simeq 690 \text{ GeV} \frac{N}{6} \sqrt{\frac{6 \text{ fb}}{\sigma(pp \to \phi \to \gamma\gamma)}}, \qquad (11)$$

$$\frac{2m_D + 3m_L}{5} \sim 80 \text{ GeV} \sqrt{\frac{6}{N}} \sqrt{\frac{\sigma(pp \to \phi \to \gamma\gamma)}{6 \text{ fb}}}, \qquad (12)$$

where we have used the reference value of the diphoton signal rate in Ref. [15] and used Eq. (9) in the second equation. The ratios of branching fractions to various ϕ decay modes are given by

$$\frac{B_{\phi \to gg}}{B_{\phi \to \gamma\gamma}} = 8 \left(\frac{6g_3^2}{14e^2} \right)^2 \simeq 200,$$

$$\frac{B_{\phi \to WW}}{B_{\phi \to \gamma\gamma}} = 2 \left(\frac{9}{14\sin^2\theta_W} \right)^2 \simeq 15,$$

$$\frac{B_{\phi \to ZZ}}{B_{\phi \to \gamma\gamma}} = \left(\frac{9 + 5\tan^4\theta_W}{14\tan^2\theta_W} \right)^2 \simeq 5,$$

$$\frac{B_{\phi \to Z\gamma}}{B_{\phi \to \gamma\gamma}} = 2 \left(\frac{9 - 5\tan^2\theta_W}{14\tan\theta_W} \right)^2 \simeq 2, \qquad (13)$$

where e and θ_W are the electromagnetic coupling and the Weinberg angle, respectively. The constraints from these decay modes [16–20] are satisfied.

Under the conditions in Eqs. (11) and (12), the masses of the other hidden pions are predicted in terms of N and the ratio $r \equiv m_D/m_L$ [6]. In the left panel of Fig. 1, we show the masses of hidden pions ψ, χ, and φ as functions of r for $N = 6$. If m_D and m_L are unified at a conventional unification scale (around $10^{14} - 10^{17}$ GeV), then their ratio at the TeV scale is in the range $r \simeq 1.5$–3, with the precise value depending on the structure of the theory above the TeV scale. In the right panel, we show these masses at $r \to \infty$ as functions of N. In drawing these plots, we have taken $\Lambda = 3.5$ TeV $\sqrt{N/6}$ motivated by Eqs. (9) and (11) and used Eq. (8) with unit coefficients. We find that the colored hidden pions ψ and χ are relatively light, $m_\psi \lesssim 1.6$ TeV and $m_\chi \lesssim 1.2$ TeV, unless N is very large, $N > 10$. We stress, however, that these masses are depicted under the assumption that $\sigma(pp \to \phi \to \gamma\gamma)_{13\text{TeV}} = 6$ fb. If this rate is smaller, then the value of f and, hence, Λ, becomes larger. This makes the hidden pion masses larger

TABLE II.   Charge assignment of the $G_H = SO(N)$ model. $\Psi_{D,L}$ and $\bar{\Psi}_{D,L}$ are left-handed Weyl spinors.

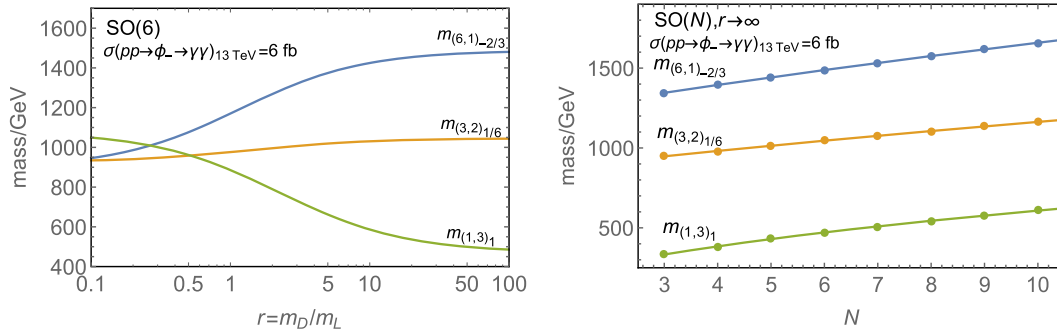|	$G_H = SO(N)$	$SU(3)_C$	$SU(2)_L$	$U(1)_Y$
Ψ_D	□	3^*	1	$1/3$
Ψ_L	□	1	2	$-1/2$
$\bar{\Psi}_D$	□	3	1	$-1/3$
$\bar{\Psi}_L$	□	1	2	$1/2$

FIG. 2.   The masses of the $(\mathbf{6},\mathbf{1})_{-2/3}$, $(\mathbf{3},\mathbf{2})_{1/6}$, and $(\mathbf{1},\mathbf{3})_1$ hidden pions appearing in the $SO(N)$ model, as functions of $r = m_D/m_L$ for $N = 6$ (left) and as functions of N for $r \to \infty$ (right).

because of larger gauge loop contributions. For detailed phenomenology of these hidden pions, see Ref. [6].

B. $G_H = SO(N)$

We now discuss the case with $G_H = SO(N)$. We assume that the hidden quarks transform as the vector representation of $SO(N)$; see Table II. The masses of the hidden quarks are given as in the $SU(N)$ case, Eq. (1). We note that the matter contents in the $SO(N)$ model discussed here and the $Sp(N)$ model discussed in the next subsection fit into representations of the $SO(10)$ grand unified group, while this is not the case for the $SU(N)$ model.

The approximate flavor symmetry of the G_H sector is now $SU(10)$. This symmetry is broken to an $SO(10)$ subgroup by the hidden quark condensations, which can again be written as Eq. (2) and do not break G_{SM}. We, therefore, have $99 - 45 = 54$ hidden pions. Specifically, in addition to ψ, χ, φ, and ϕ in Eq. (3), we have hidden pions transforming as

$$(\mathbf{6},\mathbf{1})_{-2/3}, \qquad (\mathbf{3},\mathbf{2})_{1/6}, \qquad (\mathbf{1},\mathbf{3})_1 \qquad (14)$$

under G_{SM} (which are all complex scalars). The masses of these additional hidden pions are given by

$$m^2_{(\mathbf{6},\mathbf{1})_{-2/3}} = 2m_D \frac{c}{f^2} + \frac{10}{3}\Delta_C + \frac{4}{15}\Delta_Y, \qquad (15)$$

$$m^2_{(\mathbf{3},\mathbf{2})_{1/6}} = (m_D + m_L)\frac{c}{f^2} + \frac{4}{3}\Delta_C + \frac{3}{4}\Delta_L + \frac{1}{60}\Delta_Y, \qquad (16)$$

$$m^2_{(\mathbf{1},\mathbf{3})_1} = 2m_L \frac{c}{f^2} + 2\Delta_L + \frac{3}{5}\Delta_Y, \qquad (17)$$

while those of ψ, χ, φ, and ϕ are still given by Eqs. (4)–(7).

In the left panel of Fig. 2, we show the masses of the additional hidden pions as functions of r for $N = 6$. In the right panel, we plot the masses of these hidden pions at $r \to \infty$ as functions of N. Again, we have taken $\Lambda = 3.5 \text{ TeV}\sqrt{N/6}$ and used Eq. (8) with unit

coefficients. We find that the additional colored hidden pions satisfy $m_{(\mathbf{6},\mathbf{1})_{-2/3}} \lesssim 1.7$ TeV and $m_{(\mathbf{3},\mathbf{2})_{1/6}} \lesssim 1.2$ TeV unless N is very large, $N > 10$. [These numbers assume $\sigma(pp \to \phi \to \gamma\gamma)_{13 \text{ TeV}} = 6$ fb.] All the additional hidden pions require extra interactions beyond the G_H gauge and standard model interactions to decay. If long-lived, the $(\mathbf{6},\mathbf{1})_{-2/3}$ and $(\mathbf{3},\mathbf{2})_{1/6}$ hidden pions give phenomenology similar to that of long-lived R hadrons in supersymmetric models, while the $(\mathbf{1},\mathbf{3})_1$ hidden pion gives phenomenology similar to that of long-lived sleptons.

C. $G_H = Sp(N)$

We finally discuss $G_H = Sp(N)$ (N: even).[3] We assume that the hidden quarks transform as the fundamental representation of $Sp(N)$, as in Table III. The masses of the hidden quarks are given as in Eq. (1).[4]

The approximate flavor symmetry of the G_H sector is $SU(10)$. This symmetry is broken to an $Sp(10)$ subgroup by the hidden quark condensations, which are given by Eq. (2) and do not break G_{SM}. We, therefore, have $99 - 55 = 44$ hidden pions. Specifically, in addition to ψ, χ, φ, and ϕ of the $SU(N)$ case, we have hidden pions transforming as

$$(\mathbf{3},\mathbf{1})_{2/3}, \qquad (\mathbf{3},\mathbf{2})_{1/6}, \qquad (\mathbf{1},\mathbf{1})_1 \qquad (18)$$

under G_{SM} (which are all complex scalars). The masses of these hidden pions are given by

$$m^2_{(\mathbf{3},\mathbf{1})_{2/3}} = 2m_D \frac{c}{f^2} + \frac{4}{3}\Delta_C + \frac{4}{15}\Delta_Y, \qquad (19)$$

$$m^2_{(\mathbf{3},\mathbf{2})_{1/6}} = (m_D + m_L)\frac{c}{f^2} + \frac{4}{3}\Delta_C + \frac{3}{4}\Delta_L + \frac{1}{60}\Delta_Y, \qquad (20)$$

---

[3]Our notation is such that $Sp(2) \simeq SU(2)$.
[4]If we embed G_{SM} into the $SO(10)$ grand unified group, these mass terms arise through $SO(10)$ violating effects.

TABLE III.   Charge assignment of the $G_H = Sp(N)$ model. $\Psi_{D,L}$ and $\bar{\Psi}_{D,L}$ are left-handed Weyl spinors.

	$G_H = Sp(N)$	$SU(3)_C$	$SU(2)_L$	$U(1)_Y$
Ψ_D	$\square$	$\mathbf{3^*}$	$\mathbf{1}$	$1/3$
Ψ_L	$\square$	$\mathbf{1}$	$\mathbf{2}$	$-1/2$
$\bar{\Psi}_D$	$\square$	$\mathbf{3}$	$\mathbf{1}$	$-1/3$
$\bar{\Psi}_L$	$\square$	$\mathbf{1}$	$\mathbf{2}$	$1/2$

$$m^2_{(\mathbf{1,1})_1} = 2m_L \frac{c}{f^2} + \frac{3}{5}\Delta_Y, \qquad (21)$$

while those of ψ, χ, φ, and ϕ are given by Eqs. (4)–(7).

In the left panel of Fig. 3, we show the masses of the additional hidden pions as functions of r for $N = 6$. In the right panel, we plot the masses of these hidden pions at $r \to \infty$ as functions of N. We have taken $\Lambda = 3.5$ TeV$\sqrt{N/6}$ and used Eq. (8) with unit coefficients. We find that the additional colored hidden pions satisfy $m_{(\mathbf{3,1})_{2/3}} \lesssim 1.4$ TeV and $m_{(\mathbf{3,2})_{1/6}} \lesssim 1.2$ TeV unless N is very large, $N > 10$. [The numbers are for $\sigma(pp \to \phi \to \gamma\gamma)_{13\,\text{TeV}} = 6$ fb.] Again, all the additional hidden pions require extra interactions beyond G_H gauge and standard model interactions to decay. If long-lived, the $(\mathbf{3,1})_{2/3}$ and $(\mathbf{3,2})_{1/6}$ hidden pions give phenomenology similar to that of long-lived R hadrons, while the $(\mathbf{1,1})_1$ hidden pion gives phenomenology similar to that of long-lived sleptons.

So far, we have discussed models in which $G_H = SU(N)$, $SO(N)$, and $Sp(N)$, and the hidden quarks are fundamental representations of G_H. The analysis can be easily extended to other representations. Since chiral symmetry breaking is expected to occur in the same way (other than, possibly, some special cases [21]), the physics of the hidden pions in models with hidden quarks in complex, real, and pseudoreal representations is identical to that of the models with the hidden quarks in the

fundamental representations of $G_H = SU(N)$, $SO(N)$, and $Sp(N)$, respectively.

III. MODELS WITH TWO DIPHOTON RESONANCES FROM HIDDEN PIONS

Here we consider models in which the two diphoton resonances arise from hidden pions. In Ref. [6], it was found that this can occur if the model has an extra hidden quark charged under G_H but singlet under G_{SM}. In that paper, the introduction of such an extra hidden quark was motivated by cosmology. In Sec. III A, we study the $G_H = SU(N)$ model in detail, identifying one of the two resonances as the 750 GeV diphoton resonance. In particular, we demonstrate how parameters of the models are determined and how the other hidden pion masses are predicted once the two diphoton resonances are observed. We describe $SO(N)$ and $Sp(N)$ variants in Secs. III B and III C, respectively.

A. $G_H = SU(N)$

We first discuss the case with $G_H = SU(N)$. The matter content of the model is given by Table IV, and the masses of the hidden quarks are given by

$$\mathcal{L} = -m_D \Psi_D \bar{\Psi}_D - m_L \Psi_L \bar{\Psi}_L - m_N \Psi_N \bar{\Psi}_N + \text{H.c.}, \qquad (22)$$

where we assume $m_{D,L,N} \lesssim \Lambda$.

The spectrum below Λ consists of hidden pions

$$\psi(\mathbf{8,1})_0, \qquad \chi(\mathbf{3,2})_{-5/6}, \qquad \varphi(\mathbf{1,3})_0, \qquad \phi(\mathbf{1,1})_0,$$
$$\xi(\mathbf{3,1})_{-1/3}, \qquad \lambda(\mathbf{1,2})_{1/2}, \qquad \eta(\mathbf{1,1})_0, \qquad (23)$$

where χ, ξ, and λ are complex while the others are real. Note that there are two hidden pions which are singlet under G_{SM}: one charged under $SU(5) \supset G_{SM}$, ϕ and the other singlet under it, η. The masses of the hidden pions are given by
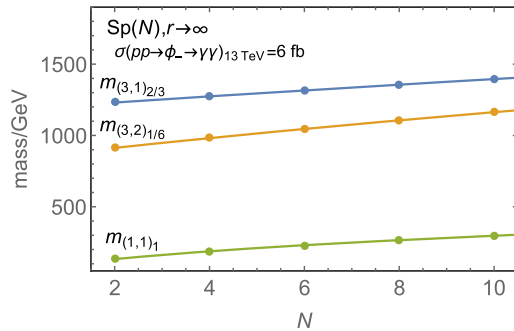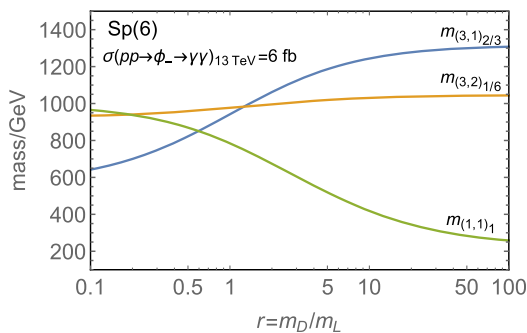

FIG. 3.   The masses of the $(\mathbf{3,1})_{2/3}$, $(\mathbf{3,2})_{1/6}$, and $(\mathbf{1,1})_1$ hidden pions appearing in the $Sp(N)$ model as functions of $r = m_D/m_L$ for $N = 6$ (left) and as functions of N for $r \to \infty$ (right).

TABLE IV. Charge assignment of the $SU(N)$ model for two diphoton resonances. $\Psi_{D,L,N}$ and $\bar{\Psi}_{D,L,N}$ are left-handed Weyl spinors.

	$G_H = SU(N)$	$SU(3)_C$	$SU(2)_L$	$U(1)_Y$
Ψ_D	□	3^*	1	1/3
Ψ_L	□	1	2	−1/2
Ψ_N	□	1	1	0
$\bar{\Psi}_D$	$\bar{\square}$	3	1	−1/3
$\bar{\Psi}_L$	$\bar{\square}$	1	2	1/2
$\bar{\Psi}_N$	$\bar{\square}$	1	1	0

$$m_\psi^2 = 2m_D \frac{c}{f^2} + 3\Delta_C, \tag{24}$$

$$m_\chi^2 = (m_D + m_L)\frac{c}{f^2} + \frac{4}{3}\Delta_C + \frac{3}{4}\Delta_L + \frac{5}{12}\Delta_Y, \tag{25}$$

$$m_\varphi^2 = 2m_L \frac{c}{f^2} + 2\Delta_L, \tag{26}$$

$$m_\xi^2 = (m_D + m_N)\frac{c}{f^2} + \frac{4}{3}\Delta_C + \frac{1}{15}\Delta_Y, \tag{27}$$

$$m_\lambda^2 = (m_L + m_N)\frac{c}{f^2} + \frac{3}{4}\Delta_L + \frac{3}{20}\Delta_Y, \tag{28}$$

$$\begin{pmatrix} m_\phi^2 & m_{\phi\eta}^2 \\ m_{\eta\phi}^2 & m_\eta^2 \end{pmatrix}$$

$$= \begin{pmatrix} \frac{2}{5}(2m_D + 3m_L) & \frac{2}{5}(m_D - m_L) \\ \frac{2}{5}(m_D - m_L) & \frac{1}{15}(3m_D + 2m_L + 25m_N) \end{pmatrix} \frac{c}{f^2}, \tag{29}$$

where c and f are the hidden quark bilinear condensate and the decay constant, respectively.

The mixing between ϕ and η vanishes for $m_D = m_L$ due to the enhanced $SU(5)$ flavor symmetry. Except for this special case, the mass eigenstates ϕ_+ and ϕ_- are determined by Eq. (29) as

$$\phi_+ = \eta \cos\theta + \phi \sin\theta, \qquad \phi_- = -\eta \sin\theta + \phi \cos\theta. \tag{30}$$

Here, the mixing angle θ and the mass eigenvalues m_+ and m_- are related with $m_{D,L,N}$ as

$$m_D = \frac{f^2}{c} \frac{m_-^2 - 3(m_+^2 - m_-^2)\tan\theta + m_+^2 \tan^2\theta}{2(1 + \tan^2\theta)}, \tag{31}$$

$$m_L = \frac{f^2}{c} \frac{m_-^2 + 2(m_+^2 - m_-^2)\tan\theta + m_+^2 \tan^2\theta}{2(1 + \tan^2\theta)}, \tag{32}$$

$$m_N = \frac{f^2}{c} \frac{6m_+^2 - m_-^2 + (m_+^2 - m_-^2)\tan\theta + (6m_-^2 - m_+^2)\tan^2\theta}{10(1 + \tan^2\theta)}. \tag{33}$$

The dimension-five couplings of the hidden pions with the standard model gauge fields are determined by chiral anomalies. The couplings of ψ, φ, and ϕ are given by Eq. (10), while those of η are given by

$$\mathcal{L} \approx \frac{Ng_3^2}{64\sqrt{15}\pi^2 f}\eta\epsilon^{\mu\nu\rho\sigma}G_{\mu\nu}^a G_{\rho\sigma}^a + \frac{Ng_2^2}{64\sqrt{15}\pi^2 f}\eta\epsilon^{\mu\nu\rho\sigma}W_{\mu\nu}^\alpha W_{\rho\sigma}^\alpha + \frac{Ng_1^2}{64\sqrt{15}\pi^2 f}\eta\epsilon^{\mu\nu\rho\sigma}B_{\mu\nu}B_{\rho\sigma}. \tag{34}$$

The couplings of the mass eigenstates $\phi_\pm$ can be read off from these expressions and the mixing in Eq. (30). By requiring that ϕ_- reproduces the 750 GeV signal

$$m_- \simeq 750 \text{ GeV}, \qquad \sigma(pp \to \phi_- \to \gamma\gamma)_{13 \text{ TeV}} \simeq 6 \text{ fb}, \tag{35}$$

we can determine the value of f as a function of the mixing angle θ between $\phi_\pm$. This is plotted in Fig. 4.

Under the conditions of Eq. (35), the properties of the second eigenstate ϕ_+ are determined by m_+ and θ. In Fig. 5, we show the contours of $\sigma(pp \to \phi_+ \to \gamma\gamma)_{13\text{TeV}}$ in the $\theta/\pi - m_+$ plane. The dark shaded region cannot
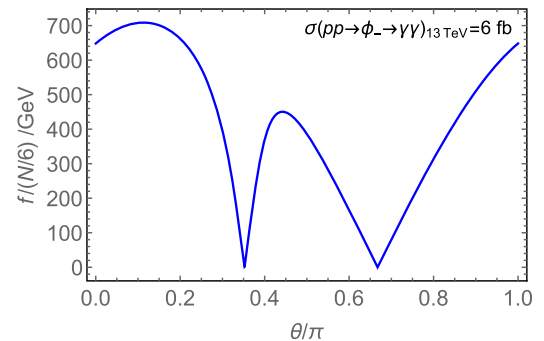

FIG. 4. The required value of the decay constant f to obtain the 750 GeV diphoton rate, $\sigma(pp \to \phi_- \to \gamma\gamma)_{13 \text{ TeV}} \simeq 6$ fb.
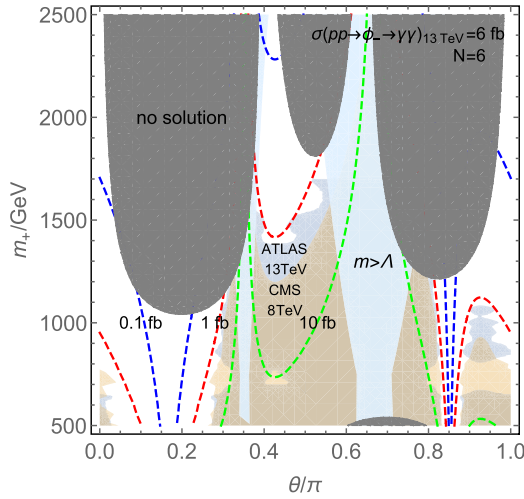
FIG. 5. Contours of $\sigma(pp \to \phi_+ \to \gamma\gamma)_{13 \text{ TeV}}$ in the $\theta/\pi - m_+$ plane under the conditions that $m_- \simeq 750$ GeV and $\sigma(pp \to \phi_- \to \gamma\gamma)_{13 \text{ TeV}} = 6$ fb. The dark shaded region cannot be obtained under $m_- \simeq 750$ GeV, while the light shaded region is either excluded by the ATLAS 13 TeV or CMS 8 TeV data or outside the regime in which the hidden pion picture is valid.

be obtained under $m_- \simeq 750$ GeV. The light shaded region is either excluded by the ATLAS [3] 13 TeV or CMS [22] 8 TeV data or outside the regime in which the hidden pion picture is valid. [As mentioned in Ref. [6], it is possible that $m_- \simeq m_+ \simeq 750$ GeV, explaining the apparent wide width of the 750 GeV excess. Our present analysis does not include this case, which requires us to take $\sigma(pp \to \phi_- \to \gamma\gamma)_{13 \text{ TeV}} < 6$ fb.]

There are two qualitatively different regions to notice. In the first region

$$-0.1(= 0.9) \lesssim \frac{\theta}{\pi} \lesssim 0.3, \tag{36}$$

ϕ_- is mostly ϕ while ϕ_+ is mostly η. In this region, we have viable parameter space for a wide range of m_+; in particular, for $0 \lesssim \theta/\pi \lesssim 0.3$, m_+ can be smaller than a TeV. The diphoton rate $\sigma(pp \to \phi_+ \to \gamma\gamma)_{13\text{TeV}}$ is of $O(0.1$–1 fb). In the second region
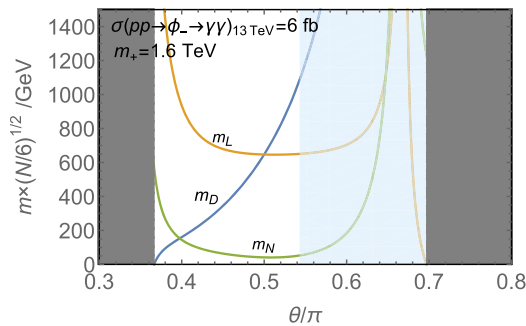
$$0.4 \lesssim \frac{\theta}{\pi} \lesssim 0.5, \tag{37}$$

the mass of ϕ_+ must be large, $m_+ \gtrsim 1.4$ TeV. In this region, the identity of the two eigenstates $\phi_\pm$ is almost opposite the case above: $\phi_- \sim \eta$ and $\phi_+ \sim \phi$. The diphoton rate $\sigma(pp \to \phi_+ \to \gamma\gamma)_{13 \text{ TeV}}$ is again of $O(0.1$–1 fb).

Below, we demonstrate if the second diphoton excess is observed, how parameters of the models are determined and how we can make further predictions. For this purpose, we choose a benchmark point from the second region, where the diphoton rate is larger than the first region for the same value of m_+. Motivated by a slight excess in the ATLAS data (although it is not significant) [1,3], we choose

$$m_+ \simeq 1.6 \text{ TeV}, \tag{38}$$

and $\theta \sim \pi/2$. In the left panel of Fig. 6, we plot the values of the hidden quark masses $m_{D,L,N}$ that reproduce Eqs. (35) and (38) as functions of θ, around $\theta \sim \pi/2$. Here, the value of the decay constant f is determined so that $\sigma(pp \to \phi_- \to \gamma\gamma) = 6$ fb is obtained at $\sqrt{s} = 13$ TeV; see Fig. 4. In the dark shaded regions, no choice of $m_{D,L,N}$ may reproduce the required $\phi_\pm$ masses. The light shaded region is excluded because of too large diphoton rates. In the right panel of Fig. 6, we plot predictions for the production cross section of ϕ_+ times the branching ratios into two electroweak gauge bosons at $\sqrt{s} = 13$ TeV. We find that the diphoton rate is indeed an observable size, as anticipated from Fig. 5. With Eqs. (35) and (38), the masses of all the other hidden pions are determined as functions of θ, as in Fig. 7. Similar analyses can be performed for any other values of m_+ once the second excess is seen.

In Fig. 7, we have also depicted the mass of the hidden η' determined by the naive scaling [23]

$$m_{\eta'} = a_1 \sqrt{\frac{6}{N}} \Lambda, \tag{39}$$

where a_1 is an $O(1)$ coefficient, and Λ is determined from f using Eq. (9). (The hidden η' mass also has a contribution
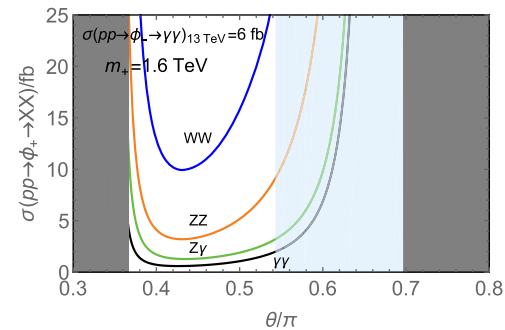

FIG. 6.   The hidden quark masses $m_{D,L,N}$ that reproduce $m_- = 750$ GeV and $m_+ = 1.6$ TeV as functions of θ (left). The production cross section of ϕ_+ times branching ratios into two electroweak gauge bosons at $\sqrt{s} = 13$ TeV (right).
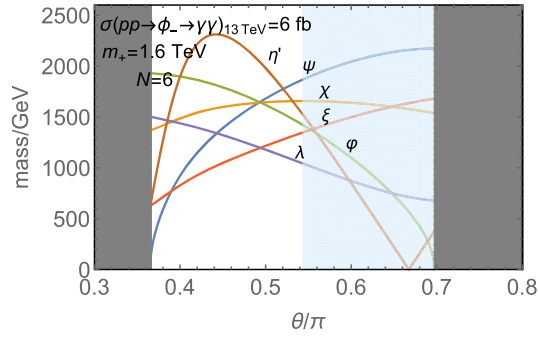
FIG. 7. The masses of hidden pions ψ, χ, φ, ξ, and λ as well as the hidden η' as functions of θ. Here, we have chosen $N = 6$.

from the hidden quark masses, which we absorb into the definition of a_1.) In the plot, we have chosen $a_1 = 1$ for definiteness. We find that the hidden η' is relatively light; this is because for $\theta \sim \pi/2$ the value of the decay constant f required to reproduce the 750 GeV excess is smaller than that for $\theta \sim 0$ (or in the model without an extra hidden quark); see Fig. 4 and Eq. (11). The couplings of the hidden η' with the standard model gauge bosons can be estimated by the $U(1)_A$ anomaly as

$$\mathcal{L} \approx \frac{Ng_3^2}{64\sqrt{3}\pi^2 f}\eta'\epsilon^{\mu\nu\rho\sigma}G_{\mu\nu}^a G_{\rho\sigma}^a + \frac{Ng_2^2}{64\sqrt{3}\pi^2 f}\eta'\epsilon^{\mu\nu\rho\sigma}W_{\mu\nu}^\alpha W_{\rho\sigma}^\alpha$$
$$+ \frac{Ng_1^2}{64\sqrt{3}\pi^2 f}\eta'\epsilon^{\mu\nu\rho\sigma}B_{\mu\nu}B_{\rho\sigma}. \quad (40)$$

(This expression is valid in the large N limit, and we expect that it gives a good approximation even for moderately large N.) In particular, the hidden η' also decays to a diphoton final state, with the rate $\sigma(pp \rightarrow \eta' \rightarrow \gamma\gamma)_{13\,\text{TeV}} \approx O(\text{fb})$. While the estimate of the hidden η' mass is subject to relatively large uncertainties, we expect from the plot that $m_{\eta'}$ is larger than m_+, at least, for some region of θ and m_+. In this case, the diphoton excess associated with η' appears above the second diphoton excess.

The relatively small value of f also implies that the dynamical scale Λ and, hence, the masses of higher resonances, are also smaller. In particular, C-odd and P-odd spin-1 resonances, which we call hidden rho mesons, have masses about Λ and are expected to be lighter than in the model without an extra hidden quark. The hidden rho mesons that have the same G_{SM} quantum numbers as the standard model gauge bosons mix with them and are singly produced at the LHC. This gives lower bounds on the hidden rho meson masses. A particularly strong bound comes from the hidden rho meson that has the same G_{SM} charges as φ, which we refer to as ρ_φ. This particle decays into an electroweak gauge boson and φ, with φ subsequently decaying into a pair of electroweak gauge bosons. (The decay of ρ_φ into a pair of φ is

kinematically forbidden.) The search for a resonance decaying into $W^\pm\gamma$ [24] excludes the ρ_φ mass smaller than about 2 TeV. While this constrains the parameter space, the model is still viable given the theoretical uncertainties associated with the estimate of the hidden rho meson masses and the fact that these masses are larger for larger N, scaling as $\sqrt{N}$ for the fixed diphoton phenomenology.

We finally mention that even if CP is not preserved in the hidden sector, the decay of ϕ_+ into two ϕ_-'s is prohibited in the limit $m_D = m_L$ because of the enhanced flavor symmetry. This limit occurs at $\theta/\pi \simeq 0.5$ for $m_+ = 1.6$ TeV; see the left panel of Fig. 6. Therefore, for such values of θ/π, the model provides the second diphoton excess from hidden pions even if CP invariance in the hidden sector is not postulated.

B. $G_H = SO(N)$

For $G_H = SO(N)$, we may add a Majorana fermion Ψ as an extra hidden quark transforming as the vector representation of $SO(N)$. Here we consider this minimal setup shown in Table V, although it is straightforward to extend the analysis in the case of multiple extra hidden quarks.

The masses of the hidden quarks are given by

$$\mathcal{L} = -m_D\Psi_D\bar{\Psi}_D - m_L\Psi_L\bar{\Psi}_L - \frac{m}{2}\Psi^2 + \text{H.c.}, \quad (41)$$

where we assume $m_{D,L}, m \lesssim \Lambda$. The hidden quark condensations

$$\langle\Psi_D\bar{\Psi}_D + \Psi_D^\dagger\bar{\Psi}_D^\dagger\rangle \approx \langle\Psi_L\bar{\Psi}_L + \Psi_L^\dagger\bar{\Psi}_L^\dagger\rangle$$
$$\approx \frac{1}{2}\langle\Psi^2 + \Psi^{\dagger 2}\rangle \equiv -c, \quad (42)$$

break the approximate $SU(11)$ flavor symmetry to $SO(11)$, so we have $120 - 55 = 65$ hidden pions. Specifically, in addition to ψ, χ, φ, ϕ, ξ, λ, and η of the $SU(N)$ case [see Eq. (23)], we have hidden pions in Eq. (14).

The physics of the diphoton resonances is essentially the same as in the $SU(N)$ case, so we can simply repeat the analysis in the case of $G_H = SU(N)$. For example, if we set $m_+ = 1.6$ TeV, the resulting hidden pion spectrum is as

TABLE V. Charge assignment of the $SO(N)$ model for two diphoton resonances. $\Psi_{D,L}$, $\bar{\Psi}_{D,L}$, and Ψ are left-handed Weyl spinors.

	$G_H = SO(N)$	$SU(3)_C$	$SU(2)_L$	$U(1)_Y$
Ψ_D	□	3^*	1	$1/3$
Ψ_L	□	1	2	$-1/2$
$\bar{\Psi}_D$	□	3	1	$-1/3$
$\bar{\Psi}_L$	□	1	2	$1/2$
Ψ	□	1	1	0

FIG. 8.   The masses of the $(\mathbf{6},\mathbf{1})_{-2/3}$, $(\mathbf{3},\mathbf{2})_{1/6}$, and $(\mathbf{1},\mathbf{3})_1$ hidden pions appearing in the $SO(N)$ model with an extra hidden quark Ψ as functions of θ for $m_+ = 1.6$ TeV.
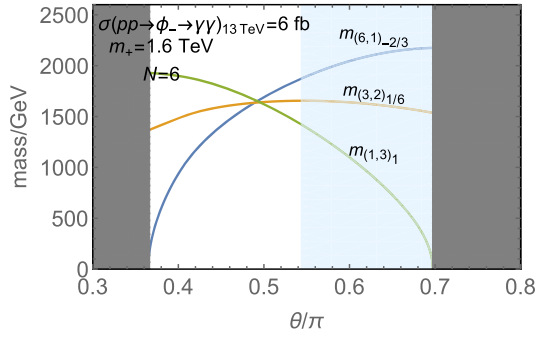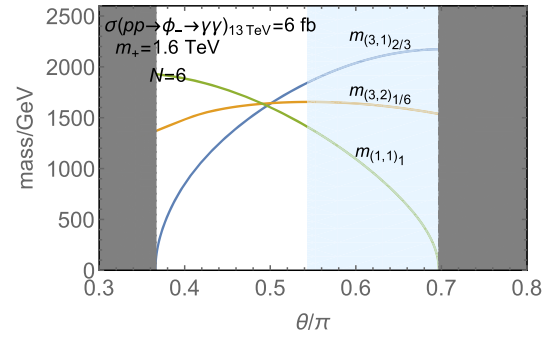

FIG. 9.   The masses of the $(\mathbf{3},\mathbf{1})_{2/3}$, $(\mathbf{3},\mathbf{2})_{1/6}$, and $(\mathbf{1},\mathbf{1})_1$ hidden pions appearing in the $Sp(N)$ model with extra hidden quarks $\Psi_{1,2}$ as functions of θ.

given in Fig. 7 for $\psi, \chi, \varphi, \phi, \xi, \lambda$, and η and in Fig. 8 for the $SO(N)$ pions of $(\mathbf{6},\mathbf{1})_{-2/3}$, $(\mathbf{3},\mathbf{2})_{1/6}$, and $(\mathbf{1},\mathbf{3})_1$.

are given in Fig. 9. The masses of ξ and ξ' and of λ and λ' are degenerate.

C. $G_H = Sp(N)$

For $G_H = Sp(N)$, the condition of global anomaly cancellation [25] requires us to introduce two Weyl fermions $\Psi_{1,2}$ that transform as the fundamental representation of $Sp(N)$. The matter content of this minimally extended model is given in Table VI.

The masses of the hidden quarks are given by

$$\mathcal{L} = -m_D \Psi_D \bar\Psi_D - m_L \Psi_L \bar\Psi_L - m \Psi_1 \Psi_2 + \text{H.c.,} \quad (43)$$

where we assume $m_{D,L}, m \lesssim \Lambda$. The hidden quark condensations

$$\langle \Psi_D \bar\Psi_D + \Psi_D^\dagger \bar\Psi_D^\dagger \rangle \approx \langle \Psi_L \bar\Psi_L + \Psi_L^\dagger \bar\Psi_L^\dagger \rangle$$
$$\approx \langle \Psi_1 \Psi_2 + \Psi_1^\dagger \Psi_2^\dagger \rangle \equiv -c, \quad (44)$$

break the approximate $SU(12)$ flavor symmetry to $Sp(12)$, so we have $143 - 78 = 65$ hidden pions. In addition to ψ, $\chi, \varphi, \phi, \xi, \lambda$, and η of the $SU(N)$ case, we now have hidden pions in Eq. (18) and one more set of ξ and λ: ξ' and λ'. The physics of the diphoton resonances is again essentially the same as in the $SU(N)$ case. For $m_+ = 1.6$ TeV, the masses of the $Sp(N)$ hidden pions $(\mathbf{3},\mathbf{1})_{2/3}$, $(\mathbf{3},\mathbf{2})_{1/6}$, and $(\mathbf{1},\mathbf{1})_1$

TABLE VI.   Charge assignment of the $Sp(N)$ model for two diphoton resonances. $\Psi_{D,L}$, $\bar\Psi_{D,L}$, and $\Psi_{1,2}$ are left-handed Weyl spinors.

	$G_H = Sp(N)$	$SU(3)_C$	$SU(2)_L$	$U(1)_Y$
Ψ_D	□	$\mathbf{3}^*$	$\mathbf{1}$	$1/3$
Ψ_L	□	$\mathbf{1}$	$\mathbf{2}$	$-1/2$
$\bar\Psi_D$	□	$\mathbf{3}$	$\mathbf{1}$	$-1/3$
$\bar\Psi_L$	□	$\mathbf{1}$	$\mathbf{2}$	$1/2$
Ψ_1	□	$\mathbf{1}$	$\mathbf{1}$	0
Ψ_2	□	$\mathbf{1}$	$\mathbf{1}$	0

D. Comment on direct couplings with the standard model

We finally comment on possible direct couplings between the hidden pions and the standard model particles. With an introduction of the singlet hidden quark $\bar\Psi_N$ (or $\Psi/\Psi_{1,2}$), we may introduce the coupling

$$\mathcal{L} = y \Psi_L \bar\Psi_N h^\dagger, \quad (45)$$

where h is the standard model Higgs field. This coupling induces mixing between the singlet pions $\phi_\pm$ and the standard model Higgs field and, hence, leads to efficient decays of the singlet pions into the standard model particles, e.g., top quarks. We assume that this coupling is sufficiently suppressed that our discussion is not affected.

IV. DECAYS OF WOULD-BE STABLE PARTICLES

The composite models we have discussed contain would-be stable particles which do not decay solely by G_H or G_{SM} gauge interactions. Unless the reheating temperature of the Universe is very small, they are abundantly produced in the early Universe.[5] If they are electrically or color charged, their lifetimes must be short enough to evade cosmological constraints. In Ref. [6], we discussed the cosmological constraints and decays of these particles for $G_H = SU(N)$. Here, we extend these analyses to the case of $SO(N)$ and $Sp(N)$. Unless otherwise stated, we consider models without standard model singlet Ψ's. We comment on the effects of the singlets occasionally.

We first consider hidden baryons. In the $Sp(N)$ models, there are no stable baryonic composite particles. This is a significant merit of the $Sp(N)$ models, since the decays of

---

[5]For discussions on the production of quasistable particles with a small reheating temperature, see, e.g., Ref. [26].

hidden baryons typically require operators with dimensions higher than those of would-be stable hidden mesons.

The $SO(N)$ models have baryonic states. We assume that $m_L < m_D$ in the following. For even N, the lightest hidden baryon is composed of $N/2$ Ψ_L and $N/2$ $\bar{\Psi}_L$ and is neutral under the standard model gauge group. Since the thermal relic abundance of this particle is small enough, it can be stable. The mass difference between the lightest hidden baryon and other low-lying hidden baryons is of order $|m_D - m_L| \approx O(100 \text{ GeV})$ or $g_{1,2,3}^2 N\Lambda/16\pi^2 \approx O(10\text{--}100 \text{ GeV})$, which is smaller than the masses of hidden pions. Thus, other low-lying hidden baryons decay into the lightest hidden baryon and standard model particles through the emission of off-shell hidden pions. Their lifetimes are as large as the lifetime of the emitted hidden pion. We discuss the lifetimes of would-be stable pions later. If we introduce a standard model singlet Ψ, then the lightest hidden baryon can be standard model gauge charged. This is evaded if the mass of Ψ, m is sufficiently larger than m_L.

For $G_H = SO(N)$ with odd N, the lightest baryon is composed of $(N+1)/2$ Ψ_L and $(N-1)/2$ $\bar{\Psi}_L$ (or vice versa), which is charged under the standard mode gauge group as $(\mathbf{1}, \mathbf{2})_{1/2}$. Although the lightest baryon is electromagnetically neutral, direct dark matter experiments put a strict upper bound on the abundance of hyper-charged particles as $n_B/s < 8 \times 10^{-18}$ [27]. The thermal abundance of the lightest hidden baryon is determined by the annihilation into hidden pions and is as large as $n_B/s \sim 10^{-16} \times (m_B/10 \text{ TeV})$, where m_B is the mass of the lightest hidden baryon. The possibility of stable hidden baryons, therefore, is excluded. The decay operators of hidden baryons depend on the size of N. For $N = 3$, there are four Fermi operators between three hidden quarks and one standard model fermion. For $N = 5$, there are operators composed of five hidden quarks and one standard model fermion. If we introduce a standard model singlet Ψ with $m \lesssim m_L$, then the lightest hidden baryon becomes standard model gauge group neutral, composed of $(N-1)/2$ Ψ_L, $(N-1)/2$ $\bar{\Psi}_L$, and one Ψ. In this case, the lightest hidden baryon can be cosmologically stable.

Next, we consider hidden pions. Hidden pions which have nonzero "D" and/or "L" numbers are would-be stable. For $G_H = SO(N)$ and $Sp(N)$, these particles can decay via the following dimension-six operators:

$$\mathcal{L} \sim \frac{1}{M_*'^2} \Psi_{\mathbf{5}}\Psi_{\mathbf{5}}\bar{\mathbf{5}}\,\bar{\mathbf{5}} + \frac{1}{M_*'^2} \Psi_{\bar{\mathbf{5}}}\Psi_{\bar{\mathbf{5}}}(\bar{\mathbf{5}}\,\bar{\mathbf{5}})^{\dagger} + \frac{1}{M_*'^2} \Psi_{\mathbf{5}}^{\dagger}\sigma^{\mu}\Psi_{\mathbf{5}}\bar{\mathbf{5}}^{\dagger}\sigma_{\mu}\bar{\mathbf{5}}$$
$$+ \frac{1}{M_*'^2} \Psi_{\bar{\mathbf{5}}}^{\dagger}\sigma^{\mu}\Psi_{\mathbf{5}}\bar{\mathbf{5}}^{\dagger}\sigma_{\mu}\bar{\mathbf{5}}, \tag{46}$$

where we have used $SU(5)$ ($\supset G_{\text{SM}}$) notation to simplify the expression. If we introduce a standard model singlet Ψ, L number is easily broken by a renormalizable interaction

between the standard model Higgs, Ψ_L, and Ψ. With this interaction, hidden pions that are would-be stable due to L number can decay even promptly.

Notably, with superparticles at a low energy scale, the first term in Eq. (46), which leads to decays of all the would-be stable hidden pions, is generated from the dimension-five superpotential term

$$W = \frac{1}{M_*} \Psi_{\mathbf{5}}\Psi_{\mathbf{5}}\bar{\mathbf{5}}\,\bar{\mathbf{5}}. \tag{47}$$

This should be contrasted with the case of $G_H = SU(N)$, in which writing down superpotential terms which have dimensions smaller than six and lead to the decay of $(\mathbf{3}, \mathbf{2})_{-5/6}$ requires an introduction of a standard model singlet hidden quark. The loop of superpartners generates the first term in Eq. (46) with

$$\frac{1}{M_*'^2} \sim \frac{g_H^2}{16\pi^2} \frac{1}{M_*\tilde{m}}, \tag{48}$$

where $\tilde{m}$ ($> \Lambda$) represents the masses of superpartners, and g_H is the G_H gauge coupling at $\tilde{m}$. The resultant lifetimes of the would-be stable hidden pions are

$$\tau \sim \left[\frac{1}{8\pi} \left(\frac{g_H^2}{16\pi^2} \frac{\sqrt{N}\Lambda^2}{4\pi M_*\tilde{m}} \right)^2 m_\pi \right]^{-1}$$
$$\sim 10^4 \text{ sec} \times \left(\frac{M_*}{10^{16} \text{ GeV}} \right)^2 \left(\frac{\tilde{m}}{10 \text{ TeV}} \right)^2 \left(\frac{N}{6} \right)^{-1}$$
$$\times \left(\frac{\Lambda}{3 \text{ TeV}} \right)^{-4} \left(\frac{m_\pi}{1 \text{ TeV}} \right)^{-1} \left(\frac{g_H}{\pi} \right)^{-4}, \tag{49}$$

where m_π represents the hidden pion masses. The colored hidden pions efficiently annihilate around the QCD phase transition era [28], and, hence, their lifetimes need only be smaller than 10^{13-15} sec [6]. This is easily satisfied. On the other hand, the noncolored hidden pions $(\mathbf{1}, \mathbf{1})_1$ and $(\mathbf{1}, \mathbf{3})_1$ annihilate only via electroweak interactions. Their abundances after freeze-out are about $\rho/s \sim 10^{-9}$ GeV. These noncolored hidden pions decay into a pair of lepton doublets through interactions in Eq. (46). If the main decay mode is into the first or second generation leptons, the constraint from the big bang nucleosynthesis requires the lifetime to be shorter than about 10^4 sec [29]. This is satisfied for $M_* \lesssim 10^{16}$ GeV. If the main decay mode is into the third generation leptons, then the lifetime should be shorter than ≈ 0.1 sec [29], requiring smaller values of M_*. Note that, as we have mentioned above, if we introduce a standard model singlet Ψ, then the $(\mathbf{1}, \mathbf{1})_1$ and $(\mathbf{1}, \mathbf{3})_1$ hidden pions can decay much more efficiently.

As discussed in Ref. [6], conformal dynamics of G_H can make M_* in Eq. (47) small even if the suppression scale at high energies M_{*0} is large. In fact, a supersymmetric $Sp(2)$ gauge theory with matter multiplets $\Psi_{D,L}$ and $\bar{\Psi}_{D,L}$ is in the

conformal window [30]. Assuming that the $Sp(2)$ gauge theory is in the conformal phase below the scale M_{CFT}, M_* is given by

$$M_* = M_{*0}\left(\frac{\tilde{m}}{M_{\text{CFT}}}\right)^{1/5}$$
$$= 4 \times 10^{-3} M_{*0}\left(\frac{\tilde{m}}{10 \text{ TeV}}\right)^{1/5}\left(\frac{M_{\text{CFT}}}{10^{16} \text{ GeV}}\right)^{-1/5}.$$
$$(50)$$

Here, we have determined the anomalous dimension of the operator $\Psi\Psi$ by requiring that the beta function of the $Sp(2)$ gauge coupling vanishes.

With conformal dynamics, dynamical scale Λ may be related with the superpartner mass scale [6]. The G_H gauge theory can be in a conformal phase above $\tilde{m}$, and as the superpartners decouple, the theory may flow into a confining phase. For $G_H = Sp(N)$ with $\Psi_{D,L}$ and $\bar{\Psi}_{D,L}$, we find $\Lambda \sim 0.1\tilde{m}$.

V. SUMMARY

In this paper, we have studied variations of models in which the diphoton excess at $\simeq 750$ GeV is explained by a composite pseudo-Nambu-Goldstone boson associated with new strong dynamics at the TeV scale. We have studied a class of models in which one or two diphoton resonances arise from the strong dynamics with the gauge group $G_H = SU(N)$, $SO(N)$, or $Sp(N)$. We have analyzed symmetry breaking patterns and hidden pion contents in these models and predicted the spectra of hidden pions under the condition that a standard model singlet hidden pion is responsible for the 750 GeV excess. We have found that $SO(N)$ and $Sp(N)$ models have extra hidden pions beyond those in the $SU(N)$ model, which can be used to discriminate among models. We have noted that the $Sp(N)$ models do not have stable baryonic composite particles, which is cosmologically favorable because making hidden baryons decay sufficiently quickly typically requires operators with very high dimensions. If the future data confirm the existence of the $\simeq 750$ GeV particle, searches of other resonances discussed in this paper would help reveal the structure of the new TeV sector responsible for the excess.

Note added.—The paper had originally been inspired by the diphoton excess reported in Refs. [1–4], which was not confirmed by data with the enlarged statistics [31,32]. The analysis presented in this paper, however, will be useful in models for other contexts which employ similar dynamics.

[1] M. Kado, ATLAS results, in *Proceedings of the ATLAS and CMS Physics Results from Run 2, CERN, Switzerland*, 2015; ATLAS Collaboration, Report No. ATLAS-CONF-2015-081, 2015.

[2] J. Olsen, CMS results, in *Proceedings of the ATLAS and CMS Physics Results from Run 2*, CERN, Switzerland, 2015; CMS Collaboration, Report No. CMS-PAS-EXO-15-004, 2015.

[3] M. Delmastro, Diphoton searches in ATLAS, in *Proceedings of the 51st Rencontres de Moriond EW 2016*, La Thuile, Italy, 2016.

[4] P. Musella, Diphoton searches in CMS, in *Proceedings of the 51st Rencontres de Moriond EW 2016*, La Thuile, Italy, March 17, 2016.

[5] K. Harigaya and Y. Nomura, Composite models for the 750 GeV diphoton excess, Phys. Lett. B **754**, 151 (2016).

[6] K. Harigaya and Y. Nomura, A composite model for the 750 GeV diphoton excess, J. High Energy Phys. 03 (2016) 091.

[7] C. Kilic, T. Okui, and R. Sundrum, Vectorlike confinement at the LHC, J. High Energy Phys. 02 (2010) 018; C. Kilic and T. Okui, The LHC phenomenology of vectorlike confinement, J. High Energy Phys. 04 (2010) 128.

[8] C.-W. Chiang, H. Fukuda, K. Harigaya, M. Ibe, and T. T. Yanagida, Diboson resonance as a portal to hidden strong dynamics, J. High Energy Phys. 11 (2015) 015; G. Cacciapaglia, A. Deandrea, and M. Hashimoto, Scalar Hint from the Diboson Excess?, Phys. Rev. Lett. **115**, 171802 (2015); H. Cai, T. Flacke, and M. Lespinasse, A composite scalar hint from di-boson resonances?, arXiv:1512.04508.

[9] Y. Nakai, R. Sato, and K. Tobioka, Footprints of new strong dynamics via anomaly, arXiv:1512.04924; R. Franceschini *et al.*, What is the gamma gamma resonance at 750 GeV?, arXiv:1512.04933; L. Bian, N. Chen, D. Liu, and J. Shu, A hidden confining world on the 750 GeV diphoton excess, arXiv:1512.05759; N. Craig, P. Draper, C. Kilic, and S. Thomas, How the $\gamma\gamma$ resonance stole Christmas, Phys. Rev. D **93**, 115023 (2016).

[10] M. Low, A. Tesi, and L.-T. Wang, A pseudoscalar decaying to photon pairs in the early LHC run 2 data, arXiv:1512.05328; B. Bellazzini, R. Franceschini, F. Sala, and J. Serra, Goldstones in diphotons, arXiv:1512.05330;

S. Matsuzaki and K. Yamawaki, 750 GeV diphoton signal from one-family walking technipion, arXiv:1512.05564; J. M. No, V. Sanz, and J. Setford, See-saw composite Higgses at the LHC: Linking naturalness to the 750 GeV di-photon resonance, arXiv:1512.05700; Y. Bai, J. Berger, and R. Lu, A 750 GeV dark pion: Cousin of a dark *G*-parity-odd WIMP, arXiv:1512.05779; A. Belyaev, G. Cacciapaglia, H. Cai, T. Flacke, A. Parolini, and H. Seródio, Singlets in composite Higgs models in light of the LHC di-photon searches, Phys. Rev. D **94**, 015004 (2016).

[11] M. Redi, A. Strumia, A. Tesi, and E. Vigiani, Di-photon resonance and dark matter as heavy pions, J. High Energy Phys. 05 (2016) 078.

[12] L. J. Hall and Y. Nomura, A finely-predicted Higgs boson mass from a finely-tuned weak scale, J. High Energy Phys. 03 (2010) 076.

[13] S. Weinberg, *The Quantum Theory of Fields* (Cambridge University Press, Cambridge, England, 1996), Vol. II.

[14] A. Manohar and H. Georgi, Chiral quarks and the non-relativistic quark model, Nucl. Phys. **B234**, 189 (1984).

[15] D. Buttazzo, A. Greljo, and D. Marzocca, Knocking on new physics' door with a scalar resonance, Eur. Phys. J. C **76**, 116 (2016); J. Ellis, S. A. R. Ellis, J. Quevillon, V. Sanz, and T. You, On the interpretation of a possible ∼750 GeV particle decaying into $\gamma\gamma$, J. High Energy Phys. 03 (2016) 176.

[16] ATLAS Collaboration, Report No. ATLAS-CONF-2016-030, 2016.

[17] G. Aad *et al.* (ATLAS Collaboration), Search for a high-mass Higgs boson decaying to a *W* boson pair in *pp* collisions at $\sqrt{s} = 8$ TeV with the ATLAS detector, J. High Energy Phys. 01 (2016) 032.

[18] G. Aad *et al.* (ATLAS Collaboration), Search for an additional, heavy Higgs boson in the $H \to ZZ$ decay channel at $\sqrt{s} = 8$ TeV in *pp* collision data with the ATLAS detector, Eur. Phys. J. C **76**, 45 (2016).

[19] M. Aaboud *et al.* (ATLAS Collaboration), Searches for heavy diboson resonances in *pp* collisions at $\sqrt{s} = 13$ TeV with the ATLAS detector, arXiv:1606.04833.

[20] M. Aaboud *et al.* (ATLAS Collaboration), Search for heavy resonances decaying to a *Z* boson and a photon in *pp* collisions at $\sqrt{s} = 13$ TeV with the ATLAS detector, arXiv:1607.06363.

[21] D. A. Kosower, Symmetry breaking patterns in pseudoreal and real gauge theories, Phys. Lett. **144B**, 215 (1984).

[22] CMS Collaboration, Report No. CMS-PAS-EXO-12-045, 2012.

[23] E. Witten, Current algebra theorems for the U(1) Goldstone boson, Nucl. Phys. **B156**, 269 (1979); G. Veneziano, U(1) without instantons, Nucl. Phys. **B159**, 213 (1979).

[24] G. Aad *et al.* (ATLAS Collaboration), Search for new resonances in $W\gamma$ and $Z\gamma$ final states in *pp* collisions at $\sqrt{s} = 8$ TeV with the ATLAS detector, Phys. Lett. B **738**, 428 (2014).

[25] E. Witten, An SU(2) anomaly, Phys. Lett. B **117B**, 324 (1982).

[26] K. Harigaya, M. Kawasaki, K. Mukaida, and M. Yamada, Dark matter production in late time reheating, Phys. Rev. D **89**, 083532 (2014).

[27] D. S. Akerib *et al.* (LUX Collaboration), Improved Limits on Scattering of Weakly Interacting Massive Particles from Reanalysis of 2013 LUX Data, Phys. Rev. Lett. **116**, 161301 (2016).

[28] J. Kang, M. A. Luty, and S. Nasri, The relic abundance of long-lived heavy colored particles, J. High Energy Phys. 09 (2008) 086; C. Jacoby and S. Nussinov, The relic abundance of massive colored particles after a late hadronic annihilation stage, arXiv:0712.2681.

[29] M. Kawasaki, K. Kohri, and T. Moroi, Big-bang nucleo-synthesis and hadronic decay of long-lived massive particles, Phys. Rev. D **71**, 083502 (2005).

[30] N. Seiberg, Electric-magnetic duality in supersymmetric non-Abelian gauge theories, Nucl. Phys. **B435**, 129 (1995).

[31] ATLAS Collaboration, Report No. ATLAS-CONF-2016-059, 2016.

[32] V. Khachatryan *et al.* (CMS Collaboration), Search for high-mass diphoton resonances in proton-proton collisions at 13 TeV and combination with 8 TeV search, arXiv:1609.02507.